Functional Characterization of Iron-Substituted Tristetraprolin-2D (TTP-2D, NUP475-2D): RNA Binding Affinity and Selectivity†

Robert C. diTargiani, Seung Jae Lee, Sarah Wassink, and Sarah L. J. Michel*

Department of Pharmaceutical Sciences, School of Pharmacy, University of Maryland, Baltimore, Maryland 21201-1180

Received April 18, 2006; Revised Manuscript Received August 2, 2006

ABSTRACT: The protein tristetraprolin (TTP, also known as NUP475 and TIS11) is a nonclassical zinc finger protein that is involved in regulating the inflammatory response. Specifically, TTP binds to AU-rich sequence elements located at the 3′-untranslated region of cytokine mRNAs forming a complex that is degraded by the exosome. The nucleic acid binding region of TTP is comprised of two $CysX_8CysX_5CysX_3His$ domains that are activated in the presence of zinc. A two-domain construct of TTP (TTP-2D) has been cloned and overexpressed in *E. coli*. TTP-2D picks up visible red coloration from the expression media, unless it is expressed under iron-restricted conditions. The iron-binding properties of TTP-2D and the effect of iron substitution on RNA recognition have been investigated. Both Fe(II) and Fe(III) bind to TTP-2D and a full titration of Fe(III) with TTP-2D revealed that this metal ion binds with micromolar affinity. Upon reconstitution of TTP-2D with either Fe(II) or Fe(III), the protein recognizes a canonical RNA-binding sequence, UUUAUUUAUUU, with nanomolar affinity. Substitution of a single adenine or both adenines results in a decreased affinity of TTP-2D for the RNA molecule, demonstrating that both Fe(II)-TTP-2D and Fe(III)-TTP-2D selectively recognize a physiologically relevant RNA sequence. The relative affinities of Fe(II)-TTP-2D and Fe(III)-TTP-2D for the series of RNA sequences mirror those observed for Zn(II)-TTP-2D and suggest that iron is a viable substitute for zinc in this protein.

The eukaryotic protein, tristetraprolin (*1*) (TTP, also known as NUP475 (*2*) and TIS11 (*3*)), belongs to a class of zinc finger proteins that share the feature of tandem $CysX_8CysX_5CysX_3His$ (CCCH) zinc-binding domains (*4*−*8*). TTP was identified from a screen for proteins induced in response to serum, insulin, and other growth factors in murine fibroblasts (*1*−*3*), where it was initially proposed to be a DNA-binding transcription factor. Subsequent research revealed that TTP is actually an RNA-binding protein. TTP binds to messenger RNA molecules involved in inflammatory response (*9*). Early information on the role of TTP in inflammatory response came from studies on mice deficient in the TTP gene. These mice rapidly developed a number of symptoms, including cachexia, arthritis, and dermatitis, which could be attributed to the overproduction of the cytokine tumor necrosis factor-α (TNFα[1]) (*10*). These symptoms could be resolved by the addition of TNFα antibodies, suggesting a direct role of TTP in the TNFα inflammatory response pathway (*10*). Additional studies revealed that TTP regulates levels of TNFα by binding to AU-rich sequence elements (ARE) located at the 3′-untranslated regions (3′UTR) of TNFα mRNAs (*9*), forming a complex that is degraded by a 3′ to 5′ exonuclease called the exosome (*11*). Subsequently, other cytokine mRNAs were shown to be regulated by TTP, including granulocyte macrophage colony-stimulating factor (GM-CSF) (*12*), interleukin-3 (IL-3) (*13*), and interleukin-2 (IL-2) (*14*) as well as the enzyme cyclooxgenase-2 (COX-2), which is involved in the development of several cancers (*15*, *16*). In all of these cases, TTP functions as a post-transcriptional regulator by binding to mRNA molecules and regulating their half-lives. Regulation of the lifetimes of cytokine mRNAs is physiologically important. If left unregulated, cytokines promote high levels of inflammation, which can lead to deleterious consequences, such as sepsis, rheumatoid arthritis, and cancer (*17*−*20*). As such, TTP has the potential to be developed as an anti-arthritic or anti-cancer agent. A recent study illustrates this potential, whereby transfection of TTP into a tumor model characterized by abnormally stable IL-3 mRNA suppressed tumor progression (*17*, *21*).

Several reports, utilizing a variety of *in vivo* and *in vitro* techniques, have identified the region of the mRNA that TTP recognizes. TTP specifically and selectively binds to the sequence UUAUUUAUU, which is a class II AU binding

† We are grateful to the University of Maryland, Baltimore for support of this research.

* Corresponding author. Phone: (410) 706-7038. Fax: (410) 706-5017. E-mail: smichel@rx.umaryland.edu.

[1] Abbreviations: ARE, AU-rich sequence element; BME, β-mercaptoethanol; CD, circular dichroism; COX-2, cyclooxygenase-2; DEPC, diethylpyrocarbonate; DTNB, 5,5′-dithiobis(2-nitrobenzoic acid); DTT, dithiothreitol; EDTA, ethylenediaminetetracetic acid; FA, fluorescence anisotropy; F_{bound}, fraction bound; F, fluorescein; GM-CSF, granulocyte-macrophage colony-stimulating factor; HEPES, 4-(2-hydroxyethyl)-1-piperazineethanesulfonic acid; HPLC, high-performance liquid chromatography; IL-3, interleukin-3; IL-2, interleukin-2; IPTG, isopropyl-beta-D-thiogalctopyranoside; K_d, dissociation constant; LB, Luria−Bertani; MALDI-TOF, matrix-assisted laser desorption ionization time-of-flight (mass spectrometry); MES, 2-(*N*-morpholino)-ethanesulfonic acid; PCR, polymerase chain reaction; r, anisotropy; ROS, reactive oxygen species; SDS−PAGE, sodium dodecyl sulfate-polyacrylamide gel electrophoresis; SELEX, systematic evolution of ligands by exponential enrichment; TFA, trifluoroacetic acid; TFIIIA, transcription factor IIIA; TNFα, tumor necrosis factor alpha; TRIS, tris(hydroxymethyl)amino methane; 3′UTR, 3′-untranslated region.

10.1021/bi060747n CCC: $33.50
Published on Web 10/21/2006

site located at the 3′UTR of the mRNA (*22*). The region of the TTP protein responsible for RNA binding is the zinc finger region (*23*). The first zinc finger domain of TTP can recognize a short RNA sequence, UUUAUUU, with micromolar affinity (*24*), whereas both zinc finger domains recognize the UUAUUUAUU sequence with nanomolar affinity (*22*, *25*, *26*). The palindromic nature of the RNA-binding sequence (*UUAUUUAUU*) suggested that each zinc finger domain would bind to a UAU motif. A recent NMR structure of TIS11D, a human homolog of TTP, bound to the RNA sequence UUAUUUAUU confirmed this hypothesis (*7*). In this structure, each zinc finger domain folds independently and recognizes a UAUU sequence using a combination of hydrogen-bonding interactions between the protein backbone and the Watson−Crick edges of the bases and stacking interactions between specific amino acid side chains and RNA bases (*7*). The secondary structural elements are limited to a short α-helix and two turns of 3_{10} helices per CCCH domain. This structure was very insightful because it demonstrated that the recognition of RNA by TIS11D (and presumably TTP) substantially differs from the recognition of DNA or RNA by classical zinc finger proteins that exhibit extensive secondary structure and utilize hydrogen bonds between specific amino acid side chains to recognize specific DNA bases (*27*). Also of note are two recent articles in which the entire TTP protein was successfully overexpressed and purified and found to be isolable as a tetramer (*28*, *29*).

In the course of expressing a variety of TTP constructs in *E. coli*, including the full-length protein, a tandem zinc finger domain, and a single zinc finger domain, we observed that the growth media turned an orange-red color. Upon lysis, the cytoplasmic extract, which contained overexpressed TTP, turned a darker red, suggesting that the protein was sequestering iron. To investigate this observation further, TTP was grown in iron-deplete minimal media, iron-replete minimal media, and iron-deplete/zinc-replete minimal media. Only the cells grown under iron-replete conditions turned red, adding further evidence that TTP was acquiring iron. The expression and purification of similar constructs of another CCCH-type zinc finger protein PIE-1, a homolog of TTP that has a very different physiological function (*30*), did not exhibit the same color changes and presumed iron sequestration (Michel, S. L. J., unpublished results). This observation led us to investigate the potential consequences of an iron-substituted TTP protein. In particular, we became interested in understanding whether TTP is capable of binding to iron (both ferric and ferrous) and how binding to iron affects the protein's RNA recognition properties and ultimately its function.

TTP is part of a larger class of proteins referred to as zinc finger proteins. These proteins share the common feature of utilizing a combination of cysteine and histidine residues to bind to zinc (*31*−*34*). Upon binding zinc, the protein folds into the proper 3D structure, allowing the protein to function. Zinc is presumed to be the correct metal ion *in vivo* because there is no energy penalty to be paid in ligand field stabilization energy (LFSE) for tetrahedral zinc(II) as there is with other open shell metal ions (*35*). Despite the energetic preference of zinc finger proteins for zinc, the presence of mixed sulfur and nitrogen donor ligands allow zinc finger proteins to bind to other divalent metal ions including iron. There are scattered literature reports in which certain zinc finger proteins have been isolated with iron in the active site. In one example, iron bound to the TFIIIA zinc finger protein was incapable of recognizing its cognate DNA (*36*). In another case, iron bound to the estrogen receptor zinc finger protein was able to recognize its cognate DNA but formed an unstable complex (*37*). A third study found that iron bound to GATA-1 zinc finger protein exhibited a higher affinity for DNA than for the zinc bound protein (*38*). These findings are intriguing because they suggest that iron can exert either a positive or a negative effect on the function of specific zinc finger proteins and raises the question, do some zinc finger proteins actually utilize iron rather than zinc *in vivo*? The functional effect of iron binding to TTP has not been studied. Because TTP is found principally in the cytoplasm during periods of inflammation when both increased levels of reactive oxygen species (ROS) and iron are observed (*39*), iron coordination to TTP may promote oxidative damage to either the protein itself or its RNA-binding partner, making this a particular interesting protein to study in terms of iron substitution (*40*, *41*).

As part of a program directed toward understanding the consequences of iron substitution in zinc finger proteins, we have cloned, overexpressed, and purified a two-domain construct of murine TTP (TTP-2D) comprised of amino acid residues 93−164 and carried out metal-binding and RNA-binding studies to determine how iron binds to TTP-2D and to assess the effect of this substitution on RNA recognition. Our studies demonstrate that both ferric and ferrous iron can bind to TTP-2D and that these iron-substituted proteins selectively recognize the physiologically relevant RNA sequence, UUUAUUUAUUU, with affinities similar to those of the zinc bound form of TTP-2D. These results are discussed in the context of a functional role for TTP.

EXPERIMENTAL PROCEDURES

Cloning and Expression of a Murine Two-Domain TTP Construct (TTP-2D). Murine-TTP cDNA was a generous gift from Dr. Mark T. Worthington (John Hopkins University School of Medicine) (*2*). The DNA-encoding TTP-2D, the zinc finger region (residues 93−164): SRYKTEL**C**RTY-S E S G R **C** R Y G A K **C** Q F A **H** G L G E L R Q A N R H P-KYKTEL**C**HKFYLQGR**C**PYGSR**C**HFI**H**NPTEDLAL) of TTP was PCR amplified and cloned into pET15b using *NcoI* and *BamHI* restriction sites. We did not use the hexahistidine tag available in this vector because it is necessary to remove this tag to study metal binding as the hexa-histidines can serve as metal-binding ligands. We were able to overexpress and purify the peptide in sufficient quantities without the incorporation of such an affinity tag. The sequence was verified by the DNA analysis facility at the Johns Hopkins University Medical Institutions.The pET15b construct containing TTP-2D was transformed into E. *coli* BL21 (DE3) cells (Novagen) and grown in Luria−Bertani (LB) medium containing 100 μg/mL ampicillin and 100 mM $ZnCl_2$ at 37 °C until mid-log phase. Typically, cell cultures were grown to 4 h postinduction with 1 mM IPTG before being harvested by centrifugation (7800*g* for 15 min at 4 °C). The cell pellets were resuspended in 8 M urea (to unfold TTP-2D) and10 mM MES buffer at pH 6 to which one-half of an EDTA-free protease inhibitor mini tablet (Roche) was added to prevent protease activity. Following lysis by French press at 1250 psi using a Thermo Spectronic French Pressure Cell

at 4 °C, the cell debris was removed by centrifugation (12100*g* for 15 min at 4 °C). The soluble fraction was loaded onto an SP-Sepharose gravity column at room temperature and allowed to equilibrate by shaking for 1 h. Apo-TTP-2D was eluted from the column by a step gradient from 0 to 2 M NaCl in 4 M urea and 10 mM MES buffer. The protein eluted at 600 mM NaCl, and SDS−PAGE was used to confirm that the protein had been purified. The cysteine thiols of the protein were reduced by adding ~10 equiv dithiothreitol (DTT) per cysteine and heating at 55 °C for 1−2 h. The protein was further purified on a nonmetallic HPLC system (Waters 626 LC system) using a Symmetry-C18 reversed-phase HPLC column with an acetonitrile gradient containing 0.1% TFA. The protein eluted from the column at 32% acetonitrile. The collected fractions were dried using a Savant SpeedVac concentrator housed in a Coy anaerobic chamber (95% nitrogen/5%hydrogen atmosphere). All further protein manipulations were performed in this atmosphere to prevent cysteine oxidation. The mass of the protein was confirmed using MALDI-TOF mass spectrometry (calculated 8581.8 Da; observed 8581.7 Da). The yield of TTP-2D was 15 mg/L of culture.

Assay for Thiols. A 5,5′-dithiobis(2-nitrobenzoic acid) (DTNB) assay was carried out to determine the number of thiols present, following the Ellman protocol (*42*, *43*). A typical experiment involved the addition of 1 μL of protein to a cuvette containing 100 μL of DTNB solution (50 mM NaOAc and 2 mM DTNB), 100 μL of 1 M Tris buffer at pH 8, and 799 μL of water. Using an extinction coefficient (ϵ) of 14150 M^{-1} cm^{-1} at 412 nm, the thiol content was calculated. All assays were performed under a 95% nitrogen/5% hydrogen atmosphere using solvents that had been degassed with helium. The expected thiol content was 6.0/protein and a typical thiol content measured for TTP-2D was 6.2/protein.

Expression of TTP-2D in Metal-Restricted Media. The procedure for expressing TTP-2D under metal restricted media followed that described in the Cloning and Expression of a Murine Two-Domain TTP Construct (TTP-2D) section, except metal-free M9 minimal media (20 mM Na_2HPO_4, 20 mM KH_2PO_4, 20 mM NH_4Cl, and 9 mM NaCl) supplemented with 2 mM $MgSO_4$, 0.1 mM $CaCl_2$, 22 mM glucose, and 1 mg/L thiamine were used instead of LB media. The expression was carried out under three conditions: (1) M9 media (iron and zinc deplete), (2) M9 media and 50 μM $FeCl_3$ (iron replete, zinc deplete), and (3) M9 media and 50 μM $ZnCl_2$ (zinc replete, iron deplete).

Metal-Binding Titrations. Metal-binding titrations were performed in quartz cuvettes with either Teflon-tops or screw caps using a Perkin-Elmer Lambda 25 UV/vis spectrometer. Titrations were carried out in 200 mM HEPES and 100 mM NaCl at pH 7.4 using metal-free reagents and water that had been purified using a MilliQ purification system and passed over Sigma chelex-resin. Upon their preparation, buffers were purged with helium to degas and transferred into a Coy inert atmospheric chamber. The following metal salts or stocks, which were stored anaerobically, were used for the titrations: $CoCl_2$ (EM Science), zinc atomic absorption standard (Aldrich; 15.2 mM Zn^{2+} in 0.9% HCl), iron (III) atomic absorption standard (Aldrich; 18.1 mM Fe^{3+} in 1.1% HCl, diluted to 10.0 mM in MeOH) and $(NH_4)_2Fe(SO_4)_2$ (Aldrich). Titrations were carried out in triplicate.

Co(II) and Zn(II) Binding. The affinity of TTP-2D for cobalt was measured by spectrophotometrically monitoring the titration of a solution of apo-TTP-2D (typically 50 μM in 1 mL buffer) with Co(II). The data was fit to a 1:1 binding equilibrium using KaliedaGraph software (Synergy software). The relative affinity of the protein for Zn(II) was determined by monitoring the displacement of Co(II) by Zn(II) following the method developed by Berg and Merkle (*35*).

Fe(III) Binding. The affinity of TTP-2D for Fe(III) was measured by spectrophotometrically monitoring the titration of a solution of apo-TTP-2D (typically 50 μM) with Fe(III). These titrations were carried out in the presence of 50 mM β-mercaptoethanol (BME) to prevent the oxidation of the cysteine thiols to disulfides (*44*). The Fe(III) stock was made as a water/MeOH (55/45) solution to solublize the Fe(III).

Fe(II) Binding. A complete titration of TTP-2D with Fe(II) was not carried out because upon addition of 8 equivalents of Fe(II), the appearance of an absorbance band around 500 nm attributable to Fe(III)-TTP-2D was detected. The UV−visible spectrum of Fe(II)-TTP-2D was obtained by adding 2 equiv of Fe(II) (to fill both CCCH sites) to 50 μM protein in the presence of 10 μM sodium dithionite to ensure that Fe(II) was completely reduced.

Oligonucleotide Probes. 3′-Fluorescein (F)-labeled RNA oligonucleotides with the sequences UUUAUUUAUUU-F, UUUGUUUAUUU-F, UUUGUUUGUUU-F, UUUUUUUUUU-F were obtained from Dharmacon Research, Inc. All oligonucleotides were purchased PAGE purified, deprotected, and desalted. Upon receipt, the oligonucleotides were resuspended in DEPC water and quantified.

RNA-Binding Studies. The binding of TTP-2D to the fluorescently labeled RNA oligonucleotides was studied by fluorescence anisotropy (FA). Measurements were taken with an ISS PC-1spectrofluorometer configured in the L format. Initially, a full excitation/emission spectrum was run to determine the optimum excitations/emission wavelengths for the experiment. The excitation wavelength/band-pass used in the experiments was 492 nm/2 nm, and the emission wavelength/band-pass was 523 nm/1 nm. In a typical experiment, a 10 nM solution of fluorescently labeled RNA in 200 mM HEPES, 100 mM NaCl, and 2 mM DTT with 0.05 mg/mL bovine serum albumin at pH 7.4 was added to a Spectrosil far-UV quartz window fluorescence cuvette (Starna Cells). The anisotropy, r, of the free RNA oligonucleotide was then measured. M-TTP-2D (M═Zn, Fe (II), and Fe(III)) was then titrated into the cuvette from a stock solution (2.0 equiv of metal, 200 mM HEPES, and 100 mM NaCl at pH 7.4) in a stepwise fashion, and the resultant change in anisotropy was recorded. The protein was added until the anisotropy values reached saturation. The data was analyzed by converting the anisotropy, *r*, to fraction bound, F_{bound} (the fraction of TTP-2D bound to RNA at a given RNA concentration), using the following equation:

$$F_{bound} = \frac{r - r_{free}}{r_{bound} - r_{free}}$$

where r_{free} is the anisotropy of the fluorescein-labeled oligonucleotide, and r_{bound} is the anisotropy of the RNA−protein complex at saturation. (Note that for one of the experiments, the total fluorescence intensity changed during

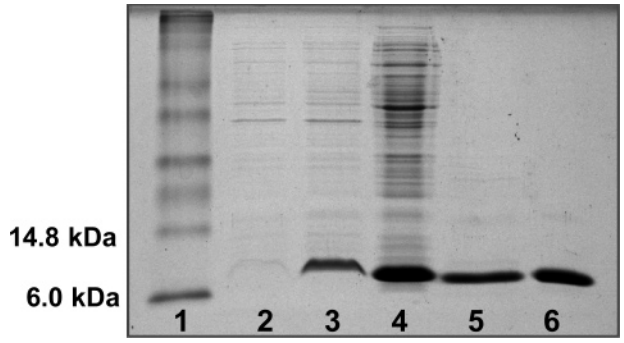

FIGURE 1: SDS−PAGE of TTP-2D stained with Coomasie Brilliant Blue during each stage of expression and purification. Lane 1, molecular weight protein standard; lane 2, uninduced protein; lane 3, induced protein; lane 4, cell lysate; lane 5, fraction from the SP Sepharose column; and lane 6, fraction from the HPLC column.

the course of the titration (Fe(III)TTP + UUUGUUUGUUU-F), and a correction factor, Q, which represents the quantum yield ratio of the bound to the free form and is calculated from the fluorescence intensity changes that occur ($Q = I_{bound} / I_{free}$), was incorporated into the equation for F_{bound}).

$$F_{bound} = \frac{r - r_{free}}{(r_{bound} - r)Q + (r - r_{free})}$$

In all cases, F_{bound} was plotted against the protein concentration and fit using the following one-site binding model

$$P + R \rightleftharpoons PR$$

$$K_d = \frac{[P][R]}{[PR]}$$

$$F_{bound} = \frac{P_{total} + R_{total} + K_d - \sqrt{(P_{total} + R_{total} + K_d)^2 - 4P_{total}R_{total}}}{2R_{total}}$$

where P is the protein (TTP-2D) concentration, and R is the RNA concentration. Each data point from the fluorescence anisotropy assay represents the average of 31 readings taken over a time course of 100 s. Each titration was carried out in triplicate.

Circular Dichroism (CD) Studies. CD spectra were recorded on a Jasco-810 spectropolarimeter. Spectral measurements were recorded at 25 °C in 10 mM Tris (pH 7.5) with 15 μM protein and 2 equivs of the appropriate metal ion. CD spectra revealed that apo-TTP-2D is completely unfolded in the absence of metal ions and adopts limited α-helical structure in their presence.

RESULTS

Protein Expression and Purification. Although a tandem zinc finger domain construct of murine TTP (mTTPDD) had been reported previously, it was of limited solubility (*45*). A soluble tandem zinc finger domain of human TIS11D, a homolog of TTP, had also been reported and was of sufficient solubility to be structurally characterized by NMR spectroscopy (*7*); therefore, we cloned and overexpressed a tandem zinc finger domain construct of murine TTP (TTP-2D) using the folded region observed in the TIS11D structure as a guide. TTP-2D was purified using a modification of the

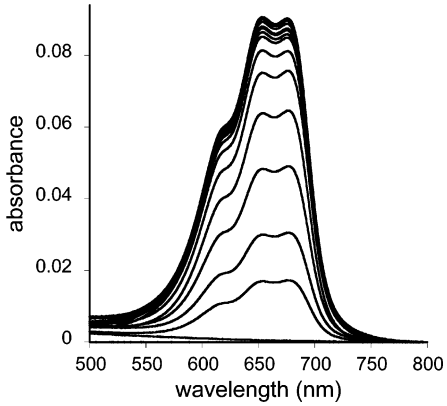

FIGURE 2: Plot of the change in the absorption spectrum between 500 and 800 nm as apo-TTP-2D is titrated with cobalt. All spectrophotometric experiments were performed in a 200 mM HEPES/100 mM NaCl buffer at pH 7.4.

protocols described for mTTPDD and TIS11D (*7*, *8*). Briefly, TTP-2D was lysed by French press under denaturing conditions (8 M urea) and purified using cation exchange chromatography (SP Sepharose) followed by reverse-phase HPLC at low pH. The isolated apo-TTP-2D peptide was lyophilized and stored aneorobically to prevent cysteine oxidation, and all subsequent manipulations were carried out under anaerobic conditions. From this procedure, 15 mg of protein was obtained per liter of cell culture and determined to be >95% pure by SDS−PAGE and analytical HPLC analysis (Figure 1). The molecular weight was confirmed by MALDI-TOF. We chose to study a fragment of TTP that contains only the zinc finger domains rather than the full-length protein (*28*, *29*) because others had demonstrated that similar fragments of close homologs could be folded and unfolded in the presence of metal ions and denaturants, respectively, and because a well-defined RNA-binding partner had been identified (*7*, *8*, *25*, *26*).

Metal-Binding Studies. To confirm that TTP-2D bound to zinc, its presumed *in vivo* cofactor, direct titrations with cobalt and competitive titrations with zinc were carried out. Zinc binding cannot be assessed directly because zinc has an electronic configuration of d^{10}. Co(II) is often used as a spectroscopic probe for zinc binding to zinc finger proteins because, like zinc, it binds to a mixed nitrogen/sulfur environment (His/Cys) in a tetrahedral coordination geometry but has the advantage of having a partially filled d-shell, d^7, which allows for d−d transitions to be optically observed (*35*, *46*). The optical spectra for a Co(II)(Cys_3His) zinc finger site is expected to exhibit d−d transitions at $\lambda = 620$, 650, and 685 nm (*8*, *24*).

Co(II) Direct Titration The titration of cobalt(II) with TTP-2D resulted in the appearance of d−d transitions in the visible region, as shown in Figure 2. The shape matches that reported for other Co(II)(Cys_3His) sites, including that reported for NUP-475DD and NUP-475D1 (a single domain) (*8*, *24*). The intensity of the d−d transitions stopped changing after the addition of 2 equivs of Co(II), indicating that cobalt binds to the two CCCH metal-binding domains of TTP-2D in a 2:1 Cobalt/TTP-2D ratio. No intermediate spectra were observed during the course of the titration, which implies that the two metal-binding sites bind cobalt with the same affinities. We were, therefore, able to fit the binding data to a 1:1 binding equilibrium by equally treating the two sites

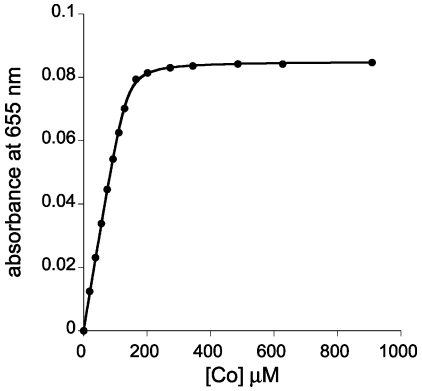

FIGURE 3: Plot of the absorption spectrum at 655 nm as a function of concentration as Co(II) is added to apo-TTP-2D. A solution of 70 μM peptide was used for this experiment, and Co (II) saturated at approximately 2 equivs. The data could be fit to yield an upper limit dissociation constant K_d of 3.3×10^{-6} M ($\pm 4 \times 10^{-7}$ M). The solid lines represent a nonlinear least-squares fit to the 1:1 binding model.

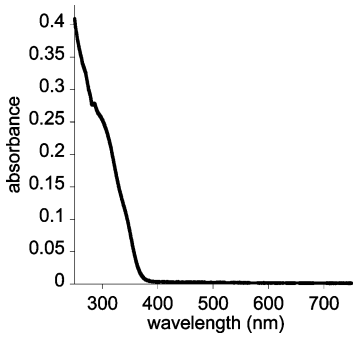

FIGURE 4: Absorption spectrum of Fe(II)-TTP-2D (200 mM HEPES/100 mM NaCl/10 μM $Na_3O_4S_2$). The spectrum was generated by subtracting the apoprotein spectrum from the metal-bound spectrum.

of TTP (*8*, *47*, *48*). Using nonlinear least-squares analysis, an upper limit dissociation constant ($K_d \geq$) of 3.3×10^{-6} M ($\pm 4 \times 10^{-7}$ M) for cobalt(II) binding and an extinction coefficient of 1254 M^{-1} (627 M^{-1} per cobalt site) at 655 nm were determined. A plot of the concentration of cobalt titrated versus absorbance, fit as described above, is shown in Figure 3.

Zn(II) Back Titration. To determine the affinity of zinc for TTP-2D, a solution of TTP-2D with a 100-fold excess of Co(II) was titrated with Zn(II), and the decrease in the Co(II)-TTP-2D absorbances were monitored. These data could be fit with the use of nonlinear least-squares analysis to yield an upper limit K_d for the Zn(II)-TTP-2D of 6.2×10^{-11} M ($\pm 6 \times 10^{-12}$ M) (*24*, *35*).

Fe(II) Binding. The addition of 2 equivs of $(NH_4)_2Fe(SO_4)_2$ to TTP-2D resulted in the appearance of bands around 290 and 338 nm (Figure 4), which we assign as charge-transfer bands on the basis of their similarity to bands observed for an iron-substituted model zinc finger protein, consensus peptide, (280 and 340 nm), reduced rubredoxin (311 and 333 nm), and models of reduced rubredoxin (310 and 332 nm) (*49*−*51*). Rubredoxin utilizes four cysteinate sulfur ligands to coordinate iron in a tetrahedral geometry and is, thus, a useful protein for spectroscopic comparison (*51*, *52*). During the course of the titration of apo-TTP-2D with Fe(II), a new broad band around 500 nm appeared. This band is indicative of an iron(III) species, implying that the addition of excess Fe(II) results in the oxidation of Fe(II)-TTP-2D (*49*).

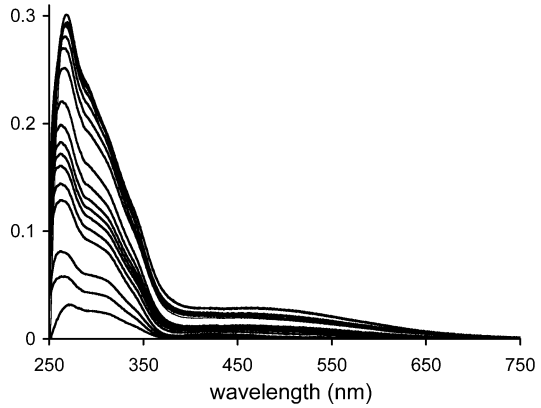

FIGURE 5: Plot in the change in the absorption spectrum between 250 and 750 nm as apo-TTP-2D is titrated with Fe(III). A solution of 40 μM peptide was used for this experiment, and Fe(III) saturated at approximately 2 equivs. The spectra were generated by subtracting the apoprotein spectrum from the metal-bound spectrum. All spectrophotometric experiments were performed in a 200 mM HEPES/100 mM NaCl/50 mM BME buffer at pH 7.4.

To determine whether Fe(II) was binding to the same site as Co(II) (and, by inference, Zn(II)), 2 equivs of Co(II) (to fill both metal-binding sites) was added to a solution of Fe(II)-TTP-2D. This resulted in the appearance of a spectrum indicative of Co(II)-TTP-2D with d−d transitions between 500 and 800 nm. The ability of Co(II) to replace Fe(II) suggests that Fe(II) binds to the same site as Co(II).

Conversion of Fe(II)-TTP-2D to Fe(III)-TTP-2D. Fe(II)-TTP-2D was crudely converted to Fe(III)-TTP-2D by exposing the Fe(II)-TTP-2D sample to air. The resultant spectrum displayed absorbances at 270, 308, and 500 nm and resembled the spectrum of oxidized rubredoxin, which exhibits a similar spectrum with red-shifted absorbances at 380, 490, and 565 nm (*50*, *52*), as well as the spectra of designed rubredoxin proteins (350, 495, and 575 nm) (*53*) and designed peptide models (*44*). This presumed Fe(III)-TTP-2D species existed for several minutes before precipitating. Ferric complexes are known to undergo hydrolysis to insoluble iron-oxide species upon exposure to oxygen, and we infer that the precipitation observed is due to this reaction (*54*).

Fe(III) Titration. To directly prepare Fe(III)-TTP-2D in a controlled manner, titrations with Fe(III) were initiated. $Fe(III)Cl_2$ is not soluble in pure water; therefore, these titrations were carried out with $Fe(III)Cl_2$ dissolved in a water/methanol solution, following an analogous procedure used by DeGrado and co-workers to study Fe(III) binding to rubredoxin peptide mimics designed *de novo* (*44*). The overall volume of methanol in the cuvette during the titration never exceeded 0.5%. The addition of iron(III) to apo-TTP-2D resulted in an optical spectrum with peaks at 270, 308, and 500 nm (Figure 5). This spectrum resembled that of oxidized rubredoxin, but the absorbances were blue-shifted compared to those observed for oxidized rubredoxin (*44*, *52*). The spectrum also matched that initially observed when Fe(II)-TTP-2D was exposed to air (*vide supra*). Fe(III) bound to TTP-2D with an upper limit K_d of 3.0×10^{-5} M ($\pm 4.0 \times 10^{-6}$ M) and was found to be highly stable when kept under strictly anaerobic conditions.

Table 1: RNA-Dissociation Constants for M-TTP-2D (M = Fe(II), Fe(III), and Zn(II))[a]

RNA sequences	Fe(II)-TTP-2D	Fe(III)-TTP-2D	Zn(II)-TTP-2D
UUUAUUUAUUU	12 ± 1	25 ± 3	16 ± 1
UUUGUUUAUUU	58 ± 4	93 ± 10	44 ± 12
UUUGUUUGUUU	205 ± 17	182 ± 15	258 ± 7
UUUUUUUUUUU	326 ± 40	253 ± 14	415 ± 45

[a] K_d is in nM.

Addition of Co(II) to Fe(III)-TTP-2D. To confirm that Fe(III) bound to the same site as Co(II) (and, by inference Zn(II)), 2 equivs of Co(II) (to fill both metal-binding sites) was added to Fe(III)-TTP-2D. This resulted in a Co(II)-TTP-2D spectrum, which suggests that Fe(III) binds to the same CCCH binding sites as those of Co(II) and Zn(II).

Fluorescence Anisotropy to Determine Binding Interactions between TTP-2D and Fluorescein-Labeled Oligonucleotides. To determine the affinities of Fe(II)-TTP-2D, Fe(III)-TTP-2D, and Zn(II)-TTP-2D for RNA, a fluorescence anisotropy assay (FA) was developed. In this assay, a solution of protein was titrated into a cuvette containing fluorescently labeled RNA and the change in anisotropy, *r*, was monitored (*55*). By varying the sequence of the RNA molecule used in the assay, the selectivity of M-TTP-2D (M═Zn(II), Fe(II), Fe(III)) for specific RNA sequences was determined. All data were fit to 1:1 binding equilibria, as described in the Experimental Procedures section.

Studies using SELEX experiments and natural binding sites have determined that the optimal binding partner for TTP is the symmetric RNA sequence UUAUUUAUU (*22*, *23*). Each UAU sequence contacts the protein and is critical for tight binding (*7*, *24*−*26*). The affinities of M-TTP-2D (M═Zn(II), Fe(II), Fe(III)) for the following RNA sequences were determined: the canonical UUUAUUUAUUU sequence and sequences in which either the adenines were substituted with either uracil or guanine, UUUUUUUUUUU, UUUGUUUGUUU, and UUUGUUUAUUU. The RNA molecules were labeled with fluorescein at the 3′-end.

Initial RNA-binding studies focused on Zn-TTP-2D to confirm that our TTP-2D construct was capable of selectively binding the canonical RNA sequence UUUAUUUAUUU. FA has been used successfully to study a single zinc finger domain of TTP (TTP-1D) (*24*) as well as a two-domain construct of human TTP (TTP) to RNA (*25*, *26*). Our studies revealed that Zn-TTP-2D bound to UUUAUUUAUUU with an affinity of 16 ± 1 nM, whereas the affinity for the altered sequences was weaker: UUUGUUUAUUU, 44 ± 12 nM; UUUGUUUGUUU, 258 ± 7 nM; and UUUUUUUUUUU, 415 ± 45 nM (Table 1). In addition, a titration of the canonical RNA sequence, UUUAUUUAUUU, with apo-TTP-2D, which is completely unfolded, resulted in precipitation, precluding further study.

Following the studies of Zn(II)-TTP-2D/RNA binding, we initiated RNA-binding studies of Fe(II)-TTP-2D with the four RNA sequences (Figure 7 shows the results of the titrations). Like Zn(II)-TTP-2D, Fe(II)-TTP-2D selectively binds to the UUUAUUUAUUU sequence with a nanomolar dissociation constant (12 ± 1 nM compared to 16 ± 1 nM for Zn). Altering the sequence by one base (UUU**G**UUUAUUU) diminishes the affinity of Fe(II)-TTP-2D for the RNA 5-fold to 58 nM (±4 nM). When two of the bases are altered,

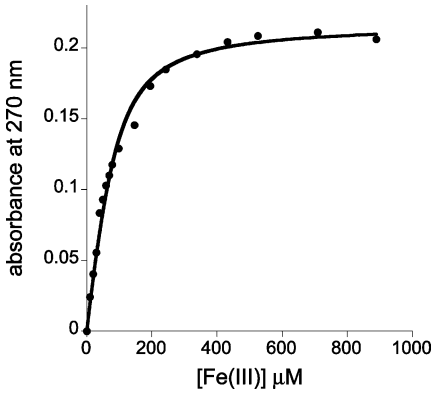

FIGURE 6: Plot of the absorption spectrum at 270 nm as a function of concentration as Fe(III) is added to apo-TTP-2D. The data could be fit to yield an upper limit dissociation constant K_d of 3.0×10^{-5} M ($\pm 4 \times 10^{-6}$ M). The solid line represents a nonlinear least-squares fit to the 1:1 binding model.

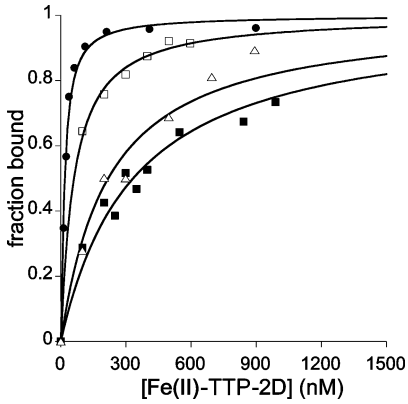

FIGURE 7: Comparison of the change in anisotropy (as fraction bound) upon the addition of Fe(II)-TTP-2D to the oligonucleotides UUUAUUUAUUU-F (●), UUUGUUUAUUU-F (□), UUUGUUUGUUU-F (△), and UUUUUUUUUUU-F (■). The solid lines represent nonlinear least-squares fits to the binding model. All FA experiments were performed in a 200 mM HEPES/100 mM NaCl/2 mM DTT buffer at pH 7.4.

UUU**G**UUU**G**UUU or UUU**U**UUU**U**UUU, the affinity decreases further to 205 nM (±17 nM) and 326 nM (±40 nM), respectively. RNA-binding studies of Fe(III)-TTP-2D with the four RNA sequences were carried out in an analogous manner, as shown in Figure 8. Fe(III)-TTP-2D also showed sequence-selective RNA binding. Fe(III)-TTP-2D binds to the canonical RNA sequence UUUAUUUAUUU with a dissociation constant of 25 nM (±3 nM) followed by a decrease to 93 nM (±10 nM) when one adenine was changed, a decrease to 182 nM (±15 nM) when both adenines were altered to guanines, and to 253 nM (±14 nM) when both adenines were altered to uracils. Table 1 lists the dissociation constants for all three proteins with all four RNA sequences. The three proteins all follow the same trend in binding, with the tightest binding observed for the physi-

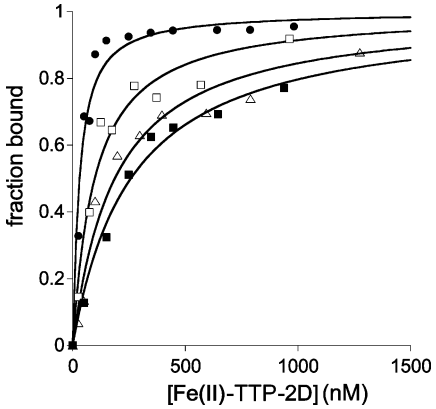

FIGURE 8: Comparison of the change in anisotropy (as fraction bound) upon the addition of Fe(III)-TTP-2D to the oligonucleotides UUUAUUUAUUU-F (●), UUUGUUUAUUU-F (□), UUUGUUUGUUU-F (△), and UUUUUUUUUUU-F (■). The solid lines represent nonlinear least-squares fits to the binding model. All FA experiments were performed in a 200 mM HEPES/100 mM NaCl/2 mM DTT buffer at pH 7.4.

ologically relevant RNA sequence, UUUAUUUAUUU, and weaker binding for the altered sequences. For all three proteins, the second tightest binding sequence was UUUGUUUAUUU. This sequence is the closest to the canonical binding sequence and contains only one base substitution (adenine to guanine). The sequences with two base substitutions exhibit even weaker binding. These results are consistent with the observation from the NMR structure of TIS11D bound to RNA that each adenine contacts the protein (*7*). Together, these results demonstrate that both ferric and ferrous iron can be substituted for zinc in TTP-2D and can selectively recognize a physiologically relevant sequence of RNA with almost the same affinity as that of the zinc-bound form of the protein.

DISCUSSION

TTP belongs to a newly emerging class of nonclassical zinc finger proteins that contain tandem CCCH metal-binding domains (*56*). The functions of these proteins range from the regulation of inflammation (i.e., TTP) (*57*) to the control of germ cell differentiation during early stages of development (i.e., PIE-1) (*30*). The CCCH residues of TTP are required for RNA binding because studies in which they have been mutated have revealed that the protein no longer binds to RNA, implying a role for these residues in metal binding (*23*). Moreover, gel-shift assays, fluorescence anisotropy, and NMR spectroscopy studies have all shown that upon the addition of zinc, TTP and some of its close homologs bind to RNA (*7*, *22*, *24*−*26*). When constructs of TTP are expressed in *E. coli* grown in rich media, the protein picks up iron, unless the cells are grown under strictly iron-deplete conditions. This iron sequestration is not observed when a homolog of TTP, PIE-1, is simultaneously expressed, raising the question, does TTP utilize iron instead of zinc *in vivo*? The goal of this study was to determine whether iron could substitute for zinc at the CCCH binding sites of TTP and, if so, to determine whether iron-substituted TTP was capable selectively binding to RNA.

Upon the purification of a two-domain construct of murine TTP, called TTP-2D, titrations of apo-TTP-2D with Co and Zn were carried out to confirm that like other TTP-derived peptides, TTP-2D binds to these metal ions with micromolar and nanomolar affinities, respectively (*8*, *24*). Upon confirmation that TTP-2D bound Co and Zn with similar affinities as those of other TTP-derived peptides, studies to examine Fe(II) and Fe(III) binding were carried out. The addition of either Fe(II) or Fe(III) to apo-TTP-2D resulted in optical spectra that resembled those of reduced and oxidized rubredoxin, respectively (*50*). Rubredoxin is a well-studied iron−sulfur protein that utilizes four cysteine ligands to bind to iron in a tetrahedral coordination geometry. On the basis of the similarities in the binding-site ligands (CCCC vs CCCH) and geometry (tetrahedral) between rubredoxin and TTP, the spectroscopic features of rubredoxin were used to understand the spectroscopy of TTP. The absorbance bands typically observed in the UV spectrum for rubredoxin are assigned as charge-transfer bands, and on the basis of spectral similarities as well as similarities in binding ligands, we tentatively assign the spectra observed for Fe(II)-TTP-2D and Fe(III)-TTP-2D as charge-transfer bands. Interestingly, the absorbance bands observed for the iron-substituted TTP-2D are blue-shifted in comparison to those observed for rubredoxin but match the absorbances observed for the iron substitution of a consensus zinc finger peptide (*49*). The air sensitivity of Fe(II) precluded a full titration of Fe(II) with TTP-2D; however, a competition experiment with Co(II)-TTP-2D demonstrated that Fe(II) binds to the same site at Co(II) and Zn(II), on the basis of the ability of Co(II) to substitute for Fe(II). A full titration of Fe(III) was carried out, and Fe(III) was found to bind to TTP-2D with an upper limit dissociation constant K_d of 30 μM. A competition experiment with Co(II) revealed that Co(II) can also replace Fe(III) and, therefore, bind at the same site.

Zinc-bound TTP-2D selectively recognizes the RNA sequence, UUUAUUUAUUU, and we utilized an FA assay to assess whether iron-substituted TTP-2D is also capable of recognizing this sequence selectively. Our FA studies revealed that both Fe(II)- and Fe(III)-TTP-2D bind to UUUAUUUAUUU selectively, and even a single base change in the sequence diminishes RNA binding. The relative affinities of Fe(II)-TTP-2D and Fe(III)-TTP-2D for the series of RNA sequences mirrors that of Zn(II)-TTP-2D, suggesting that Fe(II)-TTP-2D and Fe(III)-TTP-2D are functional alternatives to Zn(II)-TTP-2D. We were surprised that both Fe(II)- and Fe(III)-substituted TTP-2D bound to RNA with very similar affinities, given that Fe(II) is dicationic, and Fe(III) is tricationic; however, recently, Mills and Marletta observed that the ferric uptake regulator (Fur) from *E. coli* is capable of binding to its cognate DNA with either ferrous or ferric iron as a cofactor (*58*).

The ability of TTP-2D to be activated by Fe(II) and Fe(III) *in vitro* brings up the the following question: Which is the active or correct metal ion *in vivo*? Our studies have shown that although a metal is required for RNA binding, the identity of the metal ion bound to TTP-2D for RNA binding to occur is flexible. How TTP acquires metal ions *in vivo* is an open question. There has been a fair amount of debate concerning metal-ion speciation in the cell. Studies aimed at quantifying the levels of free metal ions in the cell have revealed that such levels are extremely low. For example, picomolar levels of free zinc are estimated for eukaryotes (*59*) and femtomolar levels for prokaryotes (*60*). The levels of free iron are unclear, although Outten and

O'Halloran estimate a 10^{-4} M total metal content in prokaryotic cells. These free metal ion concentrations are typically close to the K_d values reported for metal binding to specific proteins, which implies that most metal ions are sequestered by proteins. As such, it has been suggested that the metal ion occupancy should be considered in terms of kinetics rather than thermodynamics on the basis of the premise that metal ion occupancy is a dynamic, not static, process (*60*). Moreover, a thermodynamic preference for a particular metal ion does not necessarily imply that this metal ion is the correct metal ion *in vivo*; rubredoxin, for example, exhibits a thermodynamic preference for zinc, but iron is the active metal ion (*61*). Alternatively, it has been proposed that metal ion occupancy is controlled by metallochaperone proteins, and it has been suggested that specific, yet-to-be identified zinc and iron chaperone proteins, akin to those identified for copper (*62*), may regulate metal ion delivery to specific metalloproteins (*60*).

The studies reported here demonstrate that TTP-2D can coordinate different metal ions and retain functionality (i.e., its ability to bind to RNA). One may speculate that TTP may bind to different metal ions as a function of their availability in the cell. From our studies, it is not yet clear whether iron coordination is a positive or negative event. It is of interest to note that a related CCCH-type protein from *Sacharomyces cerevisiae*, Cth1, is transcriptionally induced under iron-poor conditions, whereas another CCCH-type protein from *Sacharomyces cerevisiae*, Cth2, is unaffected by iron levels, suggesting that within the family of CCCH zinc binding proteins, different members may exhibit distinct responses to metal ion levels (*63*). TTP is found in the cytoplasm during periods of inflammation, under which both iron levels and reactive oxygen species (ROS) are in abundance (*39*). As such, it may benefit TTP to coordinate iron, under these conditions, and retain functionality. The presence of the reactive oxygen species, however, suggests that iron-substituted TTP may be susceptible to oxidative damage by ROS because iron is a redox active metal. Work is currently in progress to address the susceptibility of iron-substituted TTP-2D to oxidative damage as well as to determine whether the full length TTP protein exhibits the same RNA binding properties as those of the two finger, TTP-2D, in the presence of ferric and ferrous iron.

ACKNOWLEDGMENT

We thank Mark T. Worthington of the Johns Hopkins University School of Medicine for the generous gift of TTP cDNA and Jeremy Berg, Director of NIGMS at the National Institutes of Health, Angela Wilks and Nuvjeevan Dosanjh of the University of Maryland School of Pharmacy, Department of Pharmaceutical Sciences, and Gerald Wilson of University of Maryland School of Medicine, Department of Biochemistry, for insightful discussions.

REFERENCES

1. Lai, W. S., Stumpo, D. J., and Blackshear, P. J. (1990) Rapid insulin-stimulated accumulation of an mRNA encoding a proline-rich protein, *J. Biol. Chem. 265*, 16556−16563.
2. DuBois, R. N., McLane, M. W., Ryder, K., Lau, L. F., and Nathans, D. (1990) A growth factor-inducible nuclear protein with a novel cysteine/histidine repetitive sequence, *J. Biol. Chem. 265*, 19185−19191.
3. Varnum, B. C., Ma, Q. F., Chi, T. H., Fletcher, B., and Herschman, H. R. (1991) The TIS11 primary response gene is a member of a gene family that encodes proteins with a highly conserved sequence containing an unusual Cys-His repeat, *Mol. Cell. Biol. 11*, 1754−1758.
4. Lai, W. S., Carballo, E., Thorn, J. M., Kennington, E. A., and Blackshear, P. J. (2000) Interactions of CCCH zinc finger proteins with mRNA. Binding of tristetraprolin-related zinc finger proteins to Au-rich elements and destabilization of mRNA, *J. Biol. Chem. 275*, 17827−17837.
5. Lai, W. S., Kennington, E. A., and Blackshear, P. J. (2002) Interactions of CCCH zinc finger proteins with mRNA: non-binding tristetraprolin mutants exert an inhibitory effect on degradation of AU-rich element-containing mRNAs, *J. Biol. Chem. 277*, 9606−9613.
6. Blackshear, P. J., Phillips, R. S., Vazquez-Matias, J., and Mohrenweiser, H. (2003) Polymorphisms in the genes encoding members of the tristetraprolin family of human tandem CCCH zinc finger proteins, *Prog. Nucleic Acid Res. Mol. Biol. 75*, 43−68.
7. Hudson, B. P., Martinez-Yamout, M. A., Dyson, H. J., and Wright, P. E. (2004) Recognition of the mRNA AU-rich element by the zinc finger domain of TIS11d, *Nat. Struct. Mol. Biol. 11*, 257−264.
8. Worthington, M. T., Amann, B. T., Nathans, D., and Berg, J. M. (1996) Metal binding properties and secondary structure of the zinc-binding domain of Nup475, *Proc. Natl. Acad. Sci. U.S.A. 93*, 13754−13759.
9. Carballo, E., Lai, W. S., and Blackshear, P. J. (1998) Feedback inhibition of macrophage tumor necrosis factor-alpha production by tristetraprolin, *Science 281*, 1001−1005.
10. Taylor, G. A., Carballo, E., Lee, D. M., Lai, W. S., Thompson, M. J., Patel, D. D., Schenkman, D. I., Gilkeson, G. S., Broxmeyer, H. E., Haynes, B. F., and Blackshear, P. J. (1996) A pathogenetic role for TNF alpha in the syndrome of cachexia, arthritis, and autoimmunity resulting from tristetraprolin (TTP) deficiency, *Immunity 4*, 445−454.
11. Chen, C. Y., Gherzi, R., Ong, S. E., Chan, E. L., Raijmakers, R., Pruijn, G. J., Stoecklin, G., Moroni, C., Mann, M., and Karin, M. (2001) AU binding proteins recruit the exosome to degrade ARE-containing mRNAs, *Cell 107*, 451−464.
12. Carballo, E., Lai, W. S., and Blackshear, P. J. (2000) Evidence that tristetraprolin is a physiological regulator of granulocyte-macrophage colony-stimulating factor messenger RNA deadenylation and stability, *Blood 95*, 1891−1899.
13. Stoecklin, G., Ming, X. F., Looser, R., and Moroni, C. (2000) Somatic mRNA turnover mutants implicate tristetraprolin in the interleukin-3 mRNA degradation pathway, *Mol. Cell. Biol. 20*, 3753−3763.
14. Ogilvie, R. L., Abelson, M., Hau, H. H., Vlasova, I., Blackshear, P. J., and Bohjanen, P. R. (2005) Tristetraprolin down-regulates IL-2 gene expression through AU-rich element-mediated mRNA decay, *J. Immunol. 174*, 953−961.
15. Boutaud, O., Dixon, D. A., Oates, J. A., and Sawaoka, H. (2003) Tristetraprolin binds to the COX-2 mRNA 3′ untranslated region in cancer cells, *Adv. Exp. Med. Biol. 525*, 157−160.
16. Sawaoka, H., Dixon, D. A., Oates, J. A., and Boutaud, O. (2003) Tristetraprolin binds to the 3′-untranslated region of cyclooxygenase-2 mRNA. A polyadenylation variant in a cancer cell line lacks the binding site, *J. Biol. Chem. 278*, 13928−13935.
17. Audic, Y., and Hartley, R. S. (2004) Post-transcriptional regulation in cancer, *Biol. Cell. 96*, 479−498.
18. Closa, D., and Folch-Puy, E. (2004) Oxygen free radicals and the systemic inflammatory response, *IUBMB Life 56*, 185−191.
19. Campbell, I. K., Roberts, L. J., and Wicks, I. P. (2003) Molecular targets in immune-mediated diseases: the case of tumour necrosis factor and rheumatoid arthritis, *Immunol. Cell Biol. 81*, 354−366.
20. Brown, M. A. (2005) Antibody treatments of inflammatory arthritis, *Curr. Med. Chem. 12*, 2943−2946.
21. Stoecklin, G., Gross, B., Ming, X. F., and Moroni, C. (2003) A novel mechanism of tumor suppression by destabilizing AU-rich growth factor mRNA, *Oncogene. 22*, 3554−3561.
22. Worthington, M. T., Pelo, J. W., Sachedina, M. A., Applegate, J. L., Arseneau, K. O., and Pizarro, T. T. (2002) RNA binding properties of the AU-rich element-binding recombinant Nup475/TIS11/tristetraprolin protein, *J. Biol. Chem. 277*, 48558−48564.
23. Lai, W. S., Carballo, E., Strum, J. R., Kennington, E. A., Phillips, R. S., and Blackshear, P. J. (1999) Evidence that tristetraprolin binds to AU-rich elements and promotes the deadenylation and

destabilization of tumor necrosis factor alpha mRNA, *Mol. Cell. Biol. 19*, 4311−4323.
24. Michel, S. L. J., Guerrerio, A. L., and Berg, J. M. (2003) Selective RNA binding by a single CCCH zinc-binding domain from Nup475 (Tristetraprolin), *Biochemistry 42*, 4626−4630.
25. Blackshear, P. J., Lai, W. S., Kennington, E. A., Brewer, G., Wilson, G. M., Guan, X., and Zhou, P. (2003) Characteristics of the interaction of a synthetic human tristetraprolin tandem zinc finger peptide with AU-rich element-containing RNA substrates, *J. Biol. Chem. 278*, 19947−19955.
26. Brewer, B. Y., Malicka, J., Blackshear, P. J., and Wilson, G. M. (2004) RNA sequence elements required for high affinity binding by the zinc finger domain of tristetraprolin: conformational changes coupled to the bipartite nature of Au-rich MRNA-destabilizing motifs, *J. Biol. Chem. 279*, 27870−27877.
27. Jantz, D., Amann, B. T., Gatto, G. J., Jr., and Berg, J. M. (2004) The design of functional DNA-binding proteins based on zinc finger domains, *Chem. Rev. 104*, 789−799.
28. Cao, H. (2004) Expression, purification, and biochemical characterization of the antiinflammatory tristetraprolin: a zinc-dependent mRNA binding protein affected by posttranslational modifications, *Biochemistry 43*, 13724−13738.
29. Cao, H., Dzineku, F., and Blackshear, P. J. (2003) Expression and purification of recombinant tristetraprolin that can bind to tumor necrosis factor-alpha mRNA and serve as a substrate for mitogen-activated protein kinases, *Arch. Biochem. Biophys. 412*, 106−120.
30. Tenenhaus, C., Subramaniam, K., Dunn, M. A., and Seydoux, G. (2001) PIE-1 is a bifunctional protein that regulates maternal and zygotic gene expression in the embryonic germ line of Caenorhabditis elegans, *Genes Dev. 15*, 1031−1040.
31. Berg, J. M., and Shi, Y. (1996) The galvanization of biology: a growing appreciation for the roles of zinc, *Science 271*, 1081−1085.
32. Maret, W. (2004) Zinc and sulfur: a critical biological partnership, *Biochemistry 43*, 3301−3309.
33. Matthews, J. M., and Sunde, M. (2002) Zinc fingers: folds for many occasions, *IUBMB Life 54*, 351−355.
34. Laity, J. H., Lee, B. M., and Wright, P. E. (2001) Zinc finger proteins: new insights into structural and functional diversity, *Curr. Opin. Struct. Biol. 11*, 39−46.
35. Berg, J. M., and Merkle, D. L. (1989) On the metal-ion specificity of zinc finger proteins, *J. Am. Chem. Soc. 111*, 3759−3761.
36. Hanas, J. S., Hazuda, D. J., Bogenhagen, D. F., Wu, F. Y., and Wu, C. W. (1983) Xenopus transcription factor A requires zinc for binding to the 5 S RNA gene, *J. Biol. Chem. 258*, 14120−14125.
37. Conte, D., Narindrasorasak, S., and Sarkar, B. (1996) In vivo and in vitro iron-replaced zinc finger generates free radicals and causes DNA damage, *J. Biol. Chem. 271*, 5125−5130.
38. Omichinski, J. G., Trainor, C., Evans, T., Gronenborn, A. M., Clore, G. M., and Felsenfeld, G. (1993) A small single-"finger" peptide from the erythroid transcription factor GATA-1 binds specifically to DNA as a zinc or iron complex, *Proc. Natl. Acad. Sci. U.S.A. 90*, 1676−1680.
39. Nanami, M., Ookawara, T., Otaki, Y., Ito, K., Moriguchi, R., Miyagawa, K., Hasuike, Y., Izumi, M., Eguchi, H., Suzuki, K., and Nakanishi, T. (2005) Tumor necrosis factor-alpha-induced iron sequestration and oxidative stress in human endothelial cells, *Arterioscler., Thromb., Vasc. Biol. 25*, 2495−2501.
40. Hartwig, A. (2001) Zinc finger proteins as potential targets for toxic metal ions: differential effects on structure and function, *Antioxid. Redox Signal 3*, 625−34.
41. Wilcox, D. E., Schenk, A. D., Feldman, B. M., and Xu, Y. (2001) Oxidation of zinc-binding cysteine residues in transcription factor proteins, *Antioxid. Redox Signaling 3*, 549−564.
42. Ellman, G. L. (1959) Tissue sulfhydryl groups, *Arch. Biochem. Biophys. 82*, 70−77.
43. Riddles, P. W., Blakeley, R. L., and Zerner, B. (1979) Ellman's reagent: 5, 5′-dithiobis(2-nitrobenzoic acid)−a reexamination, *Anal. Biochem. 94*, 75−81.
44. Nanda, V., Rosenblatt, M. M., Osyczka, A., Kono, H., Getahun, Z., Dutton, P. L., Saven, J. G., and Degrado, W. F. (2005) De novo design of a redox-active minimal rubredoxin mimic, *J. Am. Chem. Soc. 127*, 5804−5805.
45. Amann, B. T., Worthington, M. T., and Berg, J. M. (2003) A Cys3His zinc-binding domain from Nup475/tristetraprolin: a novel fold with a disklike structure, *Biochemistry 42*, 217−221.
46. Bertini, I., and Luchinat, C. (1984) High spin cobalt(II) as a probe for the investigation of metalloproteins, *Adv. Inorg. Biochem. 6*, 71−111.
47. Berkovits, H. J., and Berg, J. M. (1999) Metal and DNA binding properties of a two-domain fragment of neural zinc finger factor 1, a CCHC-type zinc binding protein, *Biochemistry 38*, 16826−16830.
48. Ghering, A. B., Shokes, J. E., Scott, R. A., Omichinski, J. G., and Godwin, H. A. (2004) Spectroscopic determination of the thermodynamics of cobalt and zinc binding to GATA proteins, *Biochemistry 43*, 8346−8355.
49. Krizek, B. A., and Berg, J. M. (1992) Complexes of zinc finger peptides with Ni2+ and Fe2+, *Inorg. Chem. 31*, 2984−2986.
50. Lovenberg, W., and Sobel, B. E. (1965) Rubredoxin: A new electron transfer protein from Clostridium pasteruianum, *Proc. Natl. Acad. Sci. U.S.A. 54*, 193−199.
51. Lombardi, A., Marasco, D., Maglio, O., Di C.ostanzo, L., Nastri, F., and Pavone, V. (2000) Miniaturized metalloproteins: application to iron-sulfur proteins, *Proc. Natl. Acad. Sci. U.S.A. 97*, 11922−11927.
52. Lovenberg, W., and Williams, W. M. (1969) Further observations on the chemical nature of rubredoxin from Clostridium pasteurianum, *Biochemistry 8*, 141−148.
53. Farinas, E., and Regan, L. (1998) The de novo design of a rubredoxin-like Fe site, *Protein Sci. 7*, 1939−1946.
54. Cotton, F. A., and Wilkinson, G. (1988) *Advanced Inorganic Chemistry*, 5th ed., John Wiley and Sons, New York.
55. Lakowicz, J. R. (1999) *Principles of Fluorescence Spectroscopy*, 1st ed., Kluwer Academic/Plenium Publishers, New York.
56. Hall, T. M. (2005) Multiple modes of RNA recognition by zinc finger proteins, *Curr. Opin. Struct. Biol. 15*, 367−373.
57. Blackshear, P. J. (2002) Tristetraprolin and other CCCH tandem zinc-finger proteins in the regulation of mRNA turnover, *Biochem. Soc. Trans. 30*, 945−952.
58. Mills, S. A., and Marletta, M. A. (2005) Metal binding characteristics and role of iron oxidation in the ferric uptake regulator from Escherichia coli, *Biochemistry 44*, 13553−13559.
59. Bozym, R. A., Thompson, R. B., Stoddard, A. K., and Fierke, C. A. (2006) Measuring picomolar intracellular exchangeable zinc in PC-12 cells using a ratiometric fluorescence biosensor, *ACS Chem. Biol. 1*, 103−111.
60. Outten, C. E., and O'Halloran, T. V. (2001) Femtomolar sensitivity of metalloregulatory proteins controlling zinc homeostasis, *Science 292*, 2488−2492.
61. Bonomi, F., Iametti, S., Kurtz J.r., D. M., Ragg, E. M., and Richie, K. A. (1998) Direct metal ion substitution at the [M(SCys)4]2-site of rubredoxin, *J. Biol. Inorg. Chem. 3*, 595−605.
62. Rosenzweig, A. C. (2002) Metallochaperones: bind and deliver, *Chem. Biol. 9*, 673−677.
63. Puig, S., Askeland, E., and Thiele, D. J. (2005) Coordinated remodeling of cellular metabolism during iron deficiency through targeted mRNA degradation, *Cell 120*, 99−110.

BI060747N